
Formation of Isolated Drops in a Continuous Jet

C. Bardeau^{*}, D. Fressard^{*,†}, P. Atten[†] and B. Barbet^{*,†}

^{*} Toxot Science & Applications, Bourg lès Valence, Cedex, France

[†]L.E.M.D., CNRS & Joseph Fourier University, Grenoble, Cedex, France

Introduction

With an electrohydrodynamic (EHD) generator¹, one can switch from the periodical voltage excitation to an intermittent pulse voltage stimulation. In this case, isolated drops are produced. This technique used to generate drops on demand is interesting for ink jet printing. It can as well be applied for other purposes. For instance, Hrdina and Crowley use this technique to sort biological cells². In their paper, they present a theoretical linear growth model which predicts the number of drops produced versus pulse width. But the model does not give any detail on the satellite droplets formation process. Moreover, they do not compare their predictions with experimental measurements.

Following a previous study on EHD stimulation³, this paper reports on two theoretical models of generation of isolated drops and corresponding experiments characteristic of ink-jet applications. Experimental measurements are performed with a scaled-up prototype of

an ink jet printer³. In order to validate the models, printer features such as the breakup length, the number and volume of drops and satellites produced are measured.

Our models, linear and non-linear, are both based on the Lee's equations⁴. The two models take into account a more realistic distribution of the electrostatic field than the one used by Hrdina and Crowley². The linear model gives rather accurate estimates of the variations of the breakup time. The non-linear model, which requires longer computing times, gives a good description of the drop and satellite formation.

Linear Theoretical Model

We consider a jet of conducting liquid of radius a , exiting from the nozzle with a uniform velocity U_0 , and passing through an electrode which is assumed to induce an axisymmetric field in the vicinity of the cylindrical jet interface (see Figure 1). An intermittent applied voltage of rather short duration induces a deformation of the jet on a section of spatially limited extension. This perturbation is further amplified by the capillary instability mechanism⁴, and finally leads to the formation of isolated drops.

Originally published in *Proc. of IS&T's Tenth International Congress on Advances in Non-Impact Printing Technologies*, October 30-November 4, 1994 in New Orleans, Louisiana.

This problem is examined here along the lines of a previous study of multi-electrode EHD continuous stimulation³. Since the electric field has only a limited axial extension, the process can be divided into two successive stages: a first one where the jet is subjected to the action of the electrostatic pressure, and a second stage where only the capillary forces are effective. The jet evolution can be described by the long wave cylindrical jet model proposed by Lee⁴ and previously used in EHD stimulation problems^{2,3}. In their previous study of intermittent stimulation, Hrdina and Crowley² retained a rectangular distribution of the electric field E along the axial direction. As in [3], we consider here a more realistic smooth bell-shaped axial distribution for E .

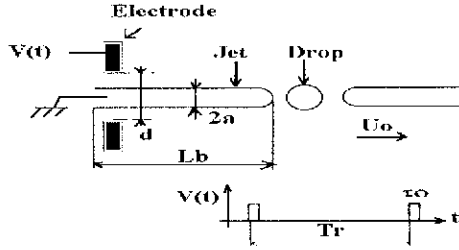


Figure 1. Schematic Representation of Isolated Drops Formation Process

Mathematical Formulation

Linearizing Lee's equations⁴ relative to an inviscid liquid, we obtain the following equation governing the surface displacement δ supposed to be very small:

$$\left[\frac{\partial}{\partial t} + U_o \frac{\partial}{\partial x} \right]^2 \delta = -\frac{T}{2\rho a} \left[\frac{\partial^2}{\partial x^2} + a^2 \frac{\partial^4}{\partial x^4} \right] \delta + \frac{a}{2\rho} \frac{\partial^2 p_e}{\partial x^2} \quad (1)$$

where T is the surface tension, ρ the mass density and p_e the electrostatic pressure. Introducing as reference scales the initial jet radius a for space variables and radius perturbation, $t_r = (\rho a^3/T)^{1/2}$ for the time and p_{eo} for the electrostatic pressure, we obtain the following equation relating the dimensionless variables:

$$\left[\frac{\partial}{\partial t} + \beta \frac{\partial}{\partial x} \right]^2 \delta = -\frac{1}{2} \left[\frac{\partial^2}{\partial x^2} + \frac{\partial^4}{\partial x^4} \right] \delta + S \frac{\partial^2 p_e}{\partial x^2} \quad (2)$$

with:

$$\beta = U_o (\rho a/T)^{1/2}, \quad S = p_{eo} a/T \quad (3)$$

β is the ratio of jet and capillary velocities, (β^2 is the Weber number), and S compares the electrostatic pressure to the capillary pressure.

The electrostatic pressure in (1) results from the action of the electric field $E(x,t)$ on the jet surface. This field can be expressed as:

$$E(x,t) = E_o f(t) g(x) \quad (4)$$

where E_o is the extremum field value, $g(x)$ represents the field variation along the axial direction (max

$|g(x)| = 1$) and $f(t)$ represents the time variation of the applied voltage. In the following, we consider only the case of rectangular pulses such that $f(t)=1$ for $0 < t < t_o$ and 0 elsewhere. The electrostatic pressure can be written:

$$p_e(x,t) = -p_{eo} G(x) \quad \text{for } 0 < t < t_o \quad (5)$$

$$p_e(x,t) = 0 \quad \text{for } t < 0 \text{ or } t > t_o$$

with $p_{eo} = 1/2 \epsilon_o E_o^2$ and $G(x) = g(x)^2$. The governing equation is then:

$$\left[\frac{\partial}{\partial t} + \beta \frac{\partial}{\partial x} \right]^2 \delta = -\frac{1}{2} \left[\frac{\partial^2}{\partial x^2} + \frac{\partial^4}{\partial x^4} \right] \delta - S \frac{\partial^2 G}{\partial x^2} \quad (6)$$

The initial conditions are such that at $t=0$

$$\delta = \frac{\partial \delta}{\partial t} = \frac{\partial \delta}{\partial x} = 0 \quad (7)$$

Typically for ink-jet applications, Weber numbers are of order $O(10^2)^3$, so it is convenient to work with the coordinates (z, τ) translating with the mean velocity of the jet. The relations between both sets of coordinates are:

$$\begin{cases} z = x - \beta t \\ \tau = t \end{cases} \quad \begin{cases} x = z + \beta \tau \\ t = \tau \end{cases} \quad (8)$$

Equation (6) then becomes:

$$\frac{\partial^2 \delta}{\partial \tau^2} = -\frac{1}{2} \left[\frac{\partial}{\partial \tau} + \frac{\partial}{\partial z} \right]^2 \delta - S \frac{\partial^2 G}{\partial z^2} (z + \beta \tau) \quad (9)$$

Jet Dynamics

During the EHD stimulation stage ($0 < \tau < \tau_o$), the deformation is very weak and in (9), the electrostatic pressure term fully dominates the capillary term which can be neglected. Equation (9) can then be integrated without knowing explicitly the function $G(x)$ for τ between 0 and τ_o (duration of voltage pulse):

$$\delta(z, \tau) = -\frac{S}{\beta^2} \left[G(z + \beta \tau) - G(z) - \beta \tau \frac{dG}{du}(z) \right] \quad (10)$$

For $\tau > \tau_o$, equation (9) reduces to the linear simplified equation for temporal instability which has simple solutions only for axially periodic deformations. The shape of $\delta(z, \tau_o)$ will change for $\tau > \tau_o$, and the way to obtain solutions is to introduce Fourier transforms (denoted by the symbol $\hat{}$), to solve (9) for every wave number and to superpose the contributions of all amplified modes ($0 < k < 1$). After some lengthy but elementary calculations, we deduce the following approximate expression valid for long enough times:

$$\delta(z, \tau) \approx \left(\frac{S}{4\pi\beta} \right) \int_0^1 (1 - \exp(ik\beta\tau_o)) \frac{\exp(\gamma_k(\tau - \tau_o))}{\gamma_k} \frac{dG}{du}(k) \exp(ikz) dk \quad (11)$$

where $k=2\pi/\lambda$ is the wave number, $\gamma_k = k[(1-k^2)/2]^{1/2}$ is the temporal growth rate and dG/du is the Fourier transform of the derivative dG/du . This relation which does not require precise knowledge of the function $G(x)$, has the advantage of giving qualitative trends. In practice due to the exponential term $\exp[\gamma_k(\tau - \tau_0)]$ in the integral, the behaviour will be controlled by a rather narrow band of wave numbers around k_{opt} corresponding to the maximum of γ_k . The factor $1 - \exp(ik\beta\tau_0)$ has a maximum norm for $k_{opt}\beta\tau_0 \approx \pi$, (modulo 2π). These jet displacement maxima correspond to minimum values of break-off length. For $k_{opt}\beta\tau_0 \approx 2\pi$ conversely, this factor is close to zero, and T_b and L_b clearly take larger values as one can note on Figure 2.

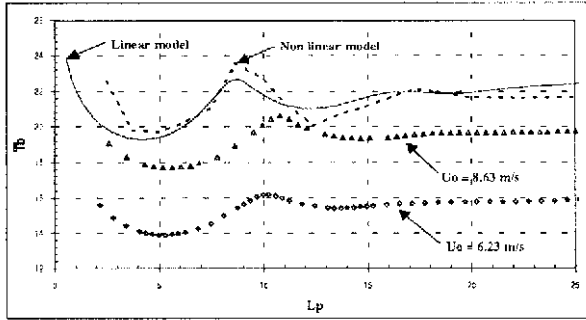


Figure 2. Dimensionless break-off time T_b versus dimensionless length of stimulated jet L_p

Breakoff Time and Drop Volume

The break-up length L_b and/or break-up time T_b can be estimated from linear theory by prescribing the perturbation amplitude to be equal to the cylindrical jet radius. The precise determination requires the knowledge of the function $G(x)$. An approximate bell-like shape for the axial variation $g(x)$ of the electric field on the cylindrical jet interface involves only simple mathematical developments:

$$g(x) = \frac{1}{2} \left(1 + \cos \pi \frac{x}{\Delta} \right) \quad -\Delta \leq x \leq \Delta \quad (12)$$

where Δ is the mid height width. The Fourier transform $d\hat{G}/du$ is then easily determined:

$$\frac{d\hat{G}}{dx}(k) = i\pi^2 h(k\Delta), \quad h(y) = \sin y \left[\frac{1}{y^2 - 4\pi^2} - \frac{1}{y^2 - \pi^2} \right] \quad (13)$$

and the break-off time T_b is the root of the equation:

$$\delta_{\min}(\tau) = -1 \quad \text{with} :$$

$$\delta_{\min}(\tau) = \min_{z>0} \frac{S\pi}{2\beta_0} \int_0^1 \sin \frac{k\beta\tau_0}{2} \cos k \left(z + \frac{\beta\tau_0}{2} \right) h(k\Delta) \frac{\exp \gamma(\tau - \tau_0)}{\gamma_k} dk \quad (14)$$

The results obtained by numerically solving (14) are plotted on Figure 2. We clearly see that the two maxima

are at the abscissae ≈ 9 and ≈ 18 respectively which correspond to the wave number of perturbation with the maximum growth rate. During the voltage pulse, the jet displacement is 9a, i.e. the wave length λ_{opt} of this perturbation with the maximum growth rate. The marked minimum is at the abscissa 4.5 which corresponds to $\lambda_{opt}/2$. Due to a “damping” effect of the modulation of T_b , the second minimum and maximum are at the abscissae about 12.5 and 17 slightly lower than $(3/2)\lambda_{opt}$ and $2\lambda_{opt}$ respectively.

The volume of isolated drops, can be estimated from the shape of the deformation, by assuming that the liquid volume between two minima of $\delta(z, \tau=T_b)$ is equal to that of the same section of the initial cylindrical jet. The results plotted in Figure 3 show that the drop volume tends to increase when the voltage pulse duration is increased up to a point where the central drop splits into two drops.

Non Linear Approach

As generally observed in the problem of stimulated jets^{3,5,6}, the linear approach leads to good estimates of the break-up length L_b , since the initial perturbations are small, i.e the linear theory is relevant. The volume of drops is only approximatively estimated by linear theory which by no means can predict the shape of the deformed jet at the break-up time.

Thus a non linear approach is required. To solve numerically the problem, we adopt a non linear approach based on one dimensional models which can be viewed as long-wave approximations of the Navier-Stokes equations. In the case of the temporal instability problem, by expanding the different variables into Fourier axial modes (truncated at some value N), the partial differential Lee equations⁴ are converted into a set of non linear ordinary differential equations which can be easily solved numerically, and give the temporal evolution of the various Fourier modes⁷. This approach has been adapted to the case of intermittent stimulation. In practice, the rectangular pulse voltage duration τ_0 is assumed to repeat with period T_r ($T_r \gg \tau_0$). The stimulation stage is treated as in the linear approach and the deformation is given by (9) at time retaining the same field distribution shape $g(x)$ as given by (12). Then this deformation is expanded into Fourier spatial modes, giving the initial conditions for integrating the non linear equations of time evolution of the various Fourier modes (up to 50 modes have been retained). Integration is stopped when the jet radius takes the value $a = 0$ at some location. The shape of the deformed jet is obtained by the temporal to spatio-temporal transformation applied in the case of high Weber number flow⁸.

The results on break-up time (Figure 2.) confirm the argument detailed at the beginning of this section: the variations of T_b are very similar to those given by the linear theory. The non linear approach is expected to account for the non linear process valid in particular for large deformations before break-up. Therefore, the non linear solution should give accurate predictions on the jet shape up to the time of first break-up. Some jet pro-

files are given in Figure 4 and we shall see in §IV that they compare favourably with experimental observations. The predictions of drop volumes would be limited in accuracy, because the integration is stopped at $t = T_b$, and it is necessary to extrapolate the long time behaviour of the strongly deformed part of the jet.

Experimental Results

Experimental Arrangement

A jet of 0.44 mm in diameter exits from a 12 mm long hypodermic needle of inner diameter $\phi = 0.45$ mm. The needle is grounded. The jet velocity U_o which can be as high as 10 m/s is controlled by a pressure regulated tank containing the fluid. The stimulation electrode consists of a stainless steel plate with a thickness of 0.2 mm. The electrode has a small hole with a diameter of 0.8 mm and the jet passes along the axis. The electrode is connected to a voltage supply with which peak amplitudes as high as 1.75 kV can be attained. A voltage pulse is generated by a micro-computer which also controls voltage period (T_r) and pulse width (τ_o). The latter can be varied between 0 and 1000 μ s with a minimum step of 10 μ s. The digital signal is converted to an analogic one to drive the High Voltage Amplifier.

The jet break-up is studied using a shadow technique described elsewhere.³ The working fluid is a glycerine-water mixture (65% glycerine) with viscosity $\eta = 17$ cps, surface tension $T = 57 \cdot 10^{-3}$ N/m and mass density $\rho = 1168$ kg/m³ at room temperature. By adding a dye, the conductivity σ of the mixture is increased to $1.6 \cdot 10^{-3}$ S/cm. Experiments are performed with a pulse voltage of 1.75 kV peak amplitude and 2816 μ s period (T_r). Breakoff length, volume of drops, and jet shape at breakoff are measured versus pulse width.

Breakoff Time Predictions and Measurements

To compare experiments to predictions, the dimensionless break-off time (T_b) is plotted versus dimensionless length of jet stimulated (L_p) in Figure 2. The dimensionless scales are calculated as following:

$$T_b = L_b / U_o T_r \quad \text{and} \quad L_p = U_o \tau_o / a.$$

The measurements have been performed at two jet velocities (6.23 and 8.63 m/s). We observe minimum and maximum values for T_b as predicted by both models.

Nevertheless, some discrepancies exist between experimental measurements and theoretical results in terms of absolute values of L_p and T_b . We attribute the difference in L_p to the fact that both theories consider an inviscid fluid. Indeed as a first approximation, by taking a growth rate modified by the effect of viscosity, the optimum wave number $k_{opt}^{(viscous)}$ ⁹ is given by:

$$k_{opt}^{(viscous)} = 1/[2(1+3O_h)]^{1/2}$$

where O_h is the Ohnesorge number $O_h = \eta/(\rho 2 a T)^{1/2}$

We obtain $k_{opt}^{(viscous)} = 0.62$ instead of 0.7 for an inviscid fluid. The former value is in better agreement with

experiments where k_{opt} (measured) is equal to 0.62 and 0.58 for respectively $U_o = 6.23$ and 8.63 m/s.

The discrepancy in the amplitude of T_b can be due to an underestimation of the electric field, and thus of the initial jet perturbation. Note that the non-linear model is not better in its predictions than the linear one as already discussed in § III.

Comparison of Volume of Drops

In Figure 3, the dimensionless drop volume (V_d) is plotted versus (L_p). Up to $L_p = 7$ (formation of a single drop), both models are in good agreement with experiments. This is probably due to the fact that in this region, the most unstable wave number is k_{opt} . For higher L_p , other wave numbers may come into play. The volume of drops increases up to a splitting into several drops of different volumes. As the calculation is stopped at the first breakoff, the volume of drops is difficult to evaluate with accuracy, since it is necessary to extrapolate the long time behaviour of the strongly deformed part of the jet. Moreover the viscous effect hinders the splitting process and this is not accounted for by the models.

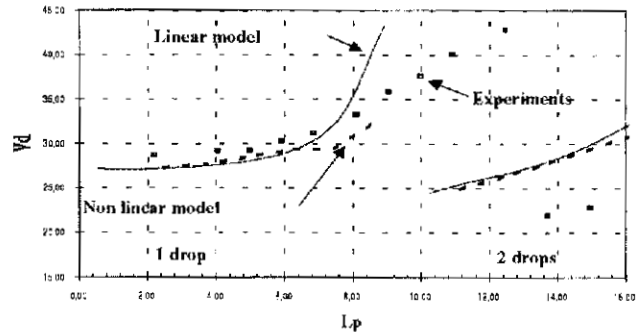


Figure 3. Dimensionless volume of drop V_d versus dimensionless length of stimulated jet L_p

In overall, the differences between the models are not very significant. Indeed, despite the fact that the non linear models accounts for the formation of satellites, its drop volume predictions are not better than the linear model ones, since the volume involved in satellites represent a few percent of drop volume.

Comparison of Breakoff Shapes

Figure 4 represents the experimental jet shapes and the non linear predictions for different dimensionless lengths L_p . For the same reason as above the predictions should only be compared with the jet shape photographs at first breakoff. There is qualitative agreement between experiments and theory. The satellite droplet formation as well as the number of drops produced could be deduced from the theoretical jet profile. However, the long time behaviour of the detached part of the jet is not easy to predict from first breakoff jet profiles. In particular, at $L_p = 12.5$, even with the photograph of the jet shape, it is difficult to decide whether or not a doubly bumped section will split into two drops.

Non linear prediction	Lp	Photographs of experimental break-off	
		First break-off	Long time behaviour
	5		
	12.5		
	13.7		
	21.5		
	24		

Figure 4. Comparison of experimental jet profiles and non linear model predictions

Conclusions

This paper presents original experiments performed on a scaled-up intermittent drop generator. The investigation includes different jet velocities and electrical pulse width voltages. Experiments confirm the predictions of two models based on the Lee's equations. The simple analytical linear model gives accurate results for breakoff length variations and volume of drop. The non linear model is derived from the expansion into Fourier modes of the jet dynamics equations, and the corresponding set of coupled non linear differential equations are solved numerically. In addition to the results obtained with the linear model, the non linear model predicts more accurately jet breakoff shapes.

Acknowledgements

We wish to thank the management of Toxot for permission to publish this paper and the Centre National de la Recherche Scientifique (CNRS) for partially funding the

study (contract CNRS/IMAJE No 50.9776). This study has also received partial financial support from the Ministère de la Recherche et de l'Enseignement Supérieur under grant No 92 P 0645.

Finally, we wish to thank A. Soucemarianadin for helpful comments.

References

1. J. M. Crowley, Electrohydrodynamic droplet generators, *J. Electrostatics*, **14**, pp. 121-134, 1983.
2. D. Hrdina and J. M. Crowley, Drop on demand operation of continuous jets using EHD techniques, *IEEE Transactions on Industry Applications*, vol. **25**, no. 4, July/August 1989.
3. A. Spohn, P. Atten, A. Soucemarianadin and A. Dunand, Theoretical and experimental study of multi-electrode electrohydrodynamic stimulation of liquid jets, *IS&T 9th Intl. Congress on Advances in Non Impact Printing Technologies*, pp. 294-297, 1993.
4. H. C. Lee, Drop formation in a liquid jet, *IBM J. Res. Develop.*, **8**, pp. 364, 1974.
5. K. C. Chaudary and T. Maxworthy, The non linear instability of a liquid jet, Part 3, *J. Fluid Mech.*, vol **96**, part 2, pp. 287-297, 1980.
6. D. F. Rutland and G. J. Jameson, *Engng. Sci.* **25**, pp. 1689, 1970.
7. S. Oliveri and P. Atten, Kinetics of charging of drops formed from a stimulated jet of conducting liquid, *IEEE Industry Applications Society Meeting Houston Texas*, pp. 1374-1380, 1992.
8. J. H. Xing, A. Boguslawski, A. Soucemarianadin, P. Atten and P. Attané, Experimental investigation of capillary instability: results on jet stimulated by pressure disturbances; paper submitted, 1994.
9. Rayleigh Lord, On the instability of a cylinder of viscous fluid under capillary forces", *Phil. Mag.*, **34**, pp. 145-154; 1892.